Theor. Comput. Fluid Dyn. (2009) 23:451–470
DOI 10.1007/s00162-009-0153-2

ORIGINAL ARTICLE

Alexander A. Chernyshov · Kirill V. Karelsky · Arakel S. Petrosyan

Validation of large eddy simulation method for study of flatness and skewness of decaying compressible magnetohydrodynamic turbulence

Received: 26 September 2008 / Accepted: 21 July 2009 / Published online: 4 September 2009

Abstract In the present work we study potential applicability of large eddy simulation (LES) method for prediction of flatness and skewness of compressible magnetohydrodynamic (MHD) turbulence. The knowledge of these quantities characterizes non-Gaussian properties of turbulence and can be used for verification of hypothesis on Gaussianity for the turbulent flow under consideration. Prediction accuracy of these quantities by means of LES method directly determines efficiency of reconstruction of probability density function (PDF) that depends on used subgrid-scale (SGS) parameterizations. Applicability of LES approach for studying of PDF properties of turbulent compressible magnetic fluid flow is investigated and potential feasibilities of five SGS parameterizations by means of comparison with direct numerical simulation results are explored. The skewness and the flatness of the velocity and the magnetic field components under various hydrodynamic Reynolds numbers, sonic Mach numbers, and magnetic Reynolds numbers are studied. It is shown that various SGS closures demonstrate the best results depending on change of similarity numbers of turbulent MHD flow. The case without any subgrid modeling yields sufficiently good results as well. This indicates that the energy pile-up at the small scales that is characteristic for the model without any subgrid closure, does not significantly influence on determination of PDF. It is shown that, among the subgrid models, the best results for studying of the flatness and the skewness of velocity and magnetic field components are demonstrated by the Smagorinsky model for MHD turbulence and the model based on cross-helicity for MHD case. It is visible from the numerical results that the influence of a choice subgrid parametrization for the flatness and the skewness of velocity is more essential than for the same characteristics of magnetic field.

Keywords Large eddy simulation · Magnetohydrodynamic turbulence · Direct numerical simulation · Flatness · Skewness · Compressible flow

PACS 95.30.Qd · 47.27.E- · 47.40.-x

1 Introduction

Studies of compressible magnetohydrodynamic (MHD) turbulence are important for understanding of processes in the space physics and astrophysics. Besides, such phenomena are widely encountered in various applied areas. For example, one can mention recent studies of the noise decrease using plasma actuator for control of large vortex structures in jets, investigations of decrease of turbulent flow resistance in aerospace industry, MHD flow in a channel for steel-casting process, and in pipes for cooling of nuclear fusion reactors. Fundamental limitations of direct numerical simulation (DNS) method for a turbulence modeling and difficulties due to presence of compressibility and magnetic field demand development of new theoretical and

A. A. Chernyshov · K. V. Karelsky · A. S. Petrosyan (✉)
Theoretical Section, Space Research Institute of the Russian Academy of Sciences, Profsoyuznaya 84/32, 117997 Moscow, Russia
E-mail: apetrosy@iki.rssi.ru

computational methods and make important advancing of large eddy simulation (LES) method for such complex MHD flows. According to LES approach, the large-scale part of the flow is computed directly and only small-scale structures of turbulence are modeled. The small-scale motion is eliminated from the initial system of equations of motion by filtering procedures and its effect is taken into account by special closures referred to as the subgrid-scale (SGS) models. In fact, LES method allows to reproduce the space–time dynamics of turbulent flow, so it is interesting to study potential possibilities of this numerical approach for computations of probability density function (PDF) which characterizes the turbulent flow [12]. The modeling results depend on characteristics of SGS models in LES method. Therefore an analysis of properties of probability density demands due caution and additional studies of applicability of various SGS parameterizations. It is known that the shape of the PDF depends on the structure of the analyzed field. In LES approach, the structure of the large eddies depends to some extent on the characteristics of the subgrid scheme and the conclusions must always be subject to cautions. Therefore, the deviation scope of probability density from Gaussian is the key characteristic of turbulent flow, since this characteristic enables to verify validity of the hypothesis about Gaussian probability density for a specific turbulent fluid flow, and to define possibility of applicability of computation results by LES method for reconstruction of PDF of a real turbulent flow. Determination accuracy of probability density may play an important role in understanding and prediction of dynamics of MHD turbulence. There are various applied and physical problems where determination accuracy of statistical properties of turbulence is principally important.

In terms of astrophysical implications, non-Gaussianity can substantially change predictions of heating of interstellar gas; mysterious structures in interstellar medium can be explained by non-Gaussian properties of MHD turbulence in the viscosity-damped regime; interaction with cosmic rays, radio waves, particle diffusion, and acceleration may be very different random flows [14]. Also this phenomenon is well documented in the laboratory. Other examples of non-Gaussianity come from the solar wind, observed in detail with a series of satellites. These and many other issues can be settled when we need better predictions non-Gaussianity of MHD turbulence.

Magnetohydrodynamic turbulence of conducting medium, unlike hydrodynamic turbulence of neutral gas, deals not only with velocity fluctuations, but also with the magnetic ones. The non-Gaussian properties of the two fields can be different. In addition, very often MHD turbulence is anisotropic. This all makes it more challenging to understand the details of PDF of MHD turbulence. Therefore, the present work concerns study of temporal dynamics of the flatness and the skewness of compressible MHD turbulence, that is related to non-Gaussianity, using LES technique.

The departure from Gaussianity for fluid turbulence in the laboratory or in numerical simulations is measured in terms of the skewness and the flatness factor. The flatness factor (sometimes also called kurtosis) in turbulent flows is a measure of non-Gaussianity. It is the fourth-order moment of the velocity field and the magnetic field, respectively:

$$Ku_j = \frac{\langle u_j^4 \rangle}{(\langle u_j^2 \rangle)^2} \tag{1}$$

$$Kb_j = \frac{\langle B_j^4 \rangle}{(\langle B_j^2 \rangle)^2}. \tag{2}$$

The flatness is an indication of the occurrence of fluctuations far from the mean: it is an indicator of the relative frequency of rare events. Hence the flatness increases with increasing sparseness of the fluctuations. Note that it represents the deviation from Gaussian in the sense that functions having large flatness values are more sharply peaked than Gaussian distributions are, and conversely.

Another interesting statistic that indicates the underlying PDF and the aspects of turbulence structure and entrainment, as well as transport is the large scale skewness. The skewness is the third-order moment of the velocity and the magnetic field. It is defined as

$$Su_j = \frac{\langle u_j^3 \rangle}{(\langle u_j^2 \rangle)^{3/2}} \tag{3}$$

$$Sb_j = \frac{\langle B_j^3 \rangle}{(\langle B_j^2 \rangle)^{3/2}} \tag{4}$$

in a temporal sense it represents the predominance of fluctuations above (positive) or below (negative) the local mean. As such it is related to the asymmetry of the PDF of the velocity or the magnetic field fluctuations. It is a sensitive indicator of changes in the large scale structure.

In the majority of cases, papers concerning LES approach for study of MHD turbulence deal with modeling MHD incompressible flows [1,11,13,16,17,23]. Recently, LES method for study of compressible MHD turbulence has been developed and cases of polytropy gas [3,4,6,7,9] and heat-conducting plasma [5,8] have been considered. In work [8] it was shown that SGS closures in the total energy equation (in the case of electrically and heat conducting fluid) do not virtually exert influence on the time dynamics of the velocity and the magnetic field and SGS models while for the temperature (same as for the internal energy) the presence of SGS models in the energy equation is an important condition for improvement of calculation accuracy of thermodynamic quantities. Therefore, without loss of generality for velocity and magnetic field, in the present paper we consider compressible MHD turbulence with the polytropic relation between density and pressure.

Limitations of DNS method for turbulence modeling especially gained momentum in studies of non-Gaussian properties of compressible MHD turbulence are well known. Therefore, it is obviously important to explore the applicability of effective approach such as LES method for studying flow properties of the charged fluid which characterize departure from Gaussianity. It is well known that filtration operation is applied in LES technique. The possibility to use filtration operations in LES method for the expansion of turbulent motion characteristics into large- and small-scale parts is due to sufficient isotropy, homogeneity, and universality of small scales of turbulent motion. The small-scale motion is eliminated from the initial system of equations of motion by using filtration procedures under the above conditions. However, use of filtering procedure in LES method actually excludes from simulation a small-scale part of turbulent flow for which just non-Gaussianity presence is typical. The question naturally arises as to whether there is a possibility of application and adequacy of LES technique for studying physical parameters which characterize non-Gaussian phenomenon. Therefore, investigation of validity of LES approach for studying of non-Gaussian compressible MHD flows is one of the objectives of the present work. For the solution of this problem, we will study and compare time dynamics of the flatness and the skewness, calculated by LES- and DNS-methods, as well as adequacy of SGS models developed earlier for modeling compressible MHD turbulence [3,7]. Also, our interest will be with the validity of LES method and SGS parameterizations depending on various similarity numbers of non-Gaussian turbulent flow.

Note that picture of turbulence is usually associated with the idea of self-similarity, or scale-invariance, which means that the spatial distribution of the turbulent eddies looks the same on any scale level in the inertial range. Nevertheless, this picture is not complete, since it ignores the existence of small-scale structures, which cannot be distributed in a uniform space-filling way. When the fluctuations of a quantity on a certain scale are not distributed in a statistically uniform way but become increasingly sparse in time or space with decreasing scale size (for example, at the dissipation scales the self-similarity is known to fail with turbulence forming non-Gaussian dissipation structures), the behavior is called intermittent and this property is called intermittency [2]. Therefore, the proposed research has prospects for studying of potential possibilities of LES technique for examination of non-Gaussian intermittent turbulent flows. However, it demands additional study.

This work is extension of our works [3,6] in which we investigated influence SGS parameterizations on time dynamics of kinetic and magnetic energy, cross-helicity, and also on spectra of magnetic and kinetic energies. LES technique has been applied to modeling compressible decaying MHD turbulence at various similarity numbers. In the whole, the best results are demonstrated by the Smagorinsky model for MHD case and the model based on cross-helicity. The scale-similarity model do not provide sufficient dissipation of both kinetic and magnetic energy, and it is necessary to use this SGS closure only together with eddy viscosity model (for example, with the Smagorinsky model), that provided a basis idea for mixed model. Aspects of applicability of various SGS models and the conclusions already obtained for the magnetic and the kinetic energies remain open for such characteristics of turbulent flow as the skewness and the flatness factor.

The present paper is organized as follows. In Sect. 2, filtered system of compressible MHD equations in dimensionless units applying the Favre-filtering operation is obtained, as well as the SGS modeling and various closure models for compressible MHD flows are specified. Section 3 is devoted to aspects of numerical

realization of LES and DNS computations. Analysis of the obtained results using numerical experiments and discussion is presented in Sect. 4. Concluding remarks are given in Sect. 5.

2 Governing equations and subgrid-scale models

In this section, we formulate the theory of LES for compressible MHDs and obtain filtered MHD equations. SGS modeling in LES is discussed and various closure models for compressible MHD case are proposed.

To obtain the MHD equations governing the motion of the filtered (that is resolved) eddies, the large scales from the small are separated. LES approach is based on the definition of a filtering operation: a resolved (or large-scale) variable, denoted by an overbar in the present paper, is defined as

$$\bar{f}(x_i) = \int_{\Theta} f(\acute{x_i}) G(x_i, \acute{x_i}; \bar{\triangle}) d\acute{x_i}, \tag{5}$$

where G is the filter function satisfying the normalization property, Θ is the domain, $\bar{\triangle}$ is the filter-width associated with the wavelength of the smallest scale retained by the filtering procedure, and $x_j = (x, y, z)$ are axes of Cartesian coordinate system.

It is convenient to use the Favre filtration (it is also called mass-weighted filtration) to avoid additional SGS terms in compressible flow. Therefore, Favre filtering will be used further on. Mass-weighted filtering is determined as follows: $\tilde{f} = \overline{\rho f}/\bar{\rho}$, where the tilde denotes the mass-weighted filtration.

Thus, applying the Favre-filtering operation, we can rewrite the MHD equations for compressible fluid flow as:

$$\frac{\partial \bar{\rho}}{\partial t} + \frac{\partial \bar{\rho} \tilde{u_j}}{\partial x_j} = 0; \tag{6}$$

$$\frac{\partial \bar{\rho} \tilde{u_i}}{\partial t} + \frac{\partial}{\partial x_j} \left(\bar{\rho} \tilde{u_i} \tilde{u_j} + \frac{\bar{\rho}^{\gamma}}{\gamma M_s^2} \delta_{ij} - \frac{1}{Re} \tilde{\sigma_{ij}} + \frac{\bar{B}^2}{2M_a^2} \delta_{ij} - \frac{1}{M_a^2} \bar{B}_j \bar{B}_i \right) = -\frac{\partial \tau_{ji}^u}{\partial x_j}; \tag{7}$$

$$\frac{\partial \bar{B}_i}{\partial t} + \frac{\partial}{\partial x_j} \left(\tilde{u_j} \bar{B}_i - \tilde{u_i} \bar{B}_j \right) - \frac{1}{Re_m} \frac{\partial^2 \bar{B}_i}{\partial x_j^2} = -\frac{\partial \tau_{ji}^b}{\partial x_j}; \tag{8}$$

$$\frac{\partial \bar{B}_j}{\partial x_j} = 0. \tag{9}$$

Here ρ is the density, u_j is the velocity in the direction x_j, B_j is the magnetic field in the direction x_j, $\sigma_{ij} = 2\mu S_{ij} - \frac{2}{3}\mu S_{kk}\delta_{ij}$ is the viscous stress tensor, $S_{ij} = 1/2 \left(\partial u_i/\partial x_j + \partial u_j/\partial x_i \right)$ is the strain rate tensor, μ is the coefficient of molecular viscosity, η is the coefficient of magnetic diffusivity, δ_{ij} is the Kronecker delta.

The filtered MHD equations (6)–(9) are written in the dimensionless form using the standard procedure [2] where $Re = \rho_0 u_0 L_0/\mu_0$ is the Reynolds number, $Re_m = u_0 L_0/\eta_0$ is the magnetic Reynolds number. $M_s = u_0/c_s$ is the Mach number, where c_s is the velocity of sound defined by the relation $c_s = \sqrt{\gamma p_0/\rho_0}$, and $M_a = u_0/u_a$ is the magnetic Mach number, where $u_a = B_0/(\sqrt{4\pi\rho_0})$ is the Alfvén velocity.

To close the Eqs. 6–8 it is assumed that the relation between density and pressure is polytropic and has the following form: $p = \rho^{\gamma}$, where γ is a polytropic index and it is supposed that $\gamma = 5/3$.

The effect of the SGSs appears on the right-hand side of the governing Eqs. 7–8 through the SGS stresses:

$$\tau_{ij}^u = \bar{\rho} \left(\widetilde{u_i u_j} - \tilde{u_i} \tilde{u_j} \right) - \frac{1}{M_a^2} \left(\overline{B_i B_j} - \bar{B}_i \bar{B}_j \right); \tag{10}$$

$$\tau_{ij}^b = \left(\overline{u_i B_j} - \tilde{u_i} \bar{B}_j \right) - \left(\overline{B_i u_j} - \bar{B}_i \tilde{u_j} \right). \tag{11}$$

Consequently, the filtered system of MHD equations contains the unknown turbulent tensors: τ_{ij}^u and τ_{ij}^b. To determine their components special turbulent closures (models, parameterizations) based on large-scale values describing turbulent MHD flow must be used. The main idea of any SGS closures used in LES is to reproduce the effects of the SGS dynamics on the large-scale energy distribution, at that as a matter of fact

Richardson turbulent cascade is simulated. In order to close the system of MHD equations we should find such parameterizations for τ^u_{ij} and τ^b_{ij} that would relate these tensors to the known large-scale values of the flow parameters.

In this paper we consider five SGS models and three of them (the Smagorinsky model for MHD case, Kolmogorov model for MHD-turbulence, model based on cross-helicity) use eddy-viscosity assumption to try to simulate the diffusive transport and dissipation of kinetic and magnetic energy. One of them (scale-similar model) is based on the assumption that the most active SGSs are those closer to the cutoff, and that the scales with which they interact are those immediately above the cutoff wave number. Also, the last SGS closures considered in present work are mixed model for MHD turbulence.

The first model is the well-known Smagorinsky model [20,22]. In this article we represent its extension to the MHD-case for compressible turbulence [6], given by

$$\tau^u_{ij} - \frac{1}{3}\tau^u_{kk}\delta_{ij} = -2C_1\bar{\rho}\bar{\triangle}^2|\tilde{S^u}|\left(\tilde{S_{ij}} - \frac{1}{3}\tilde{S_{kk}}\delta_{ij}\right), \tag{12}$$

$$\tau^b_{ij} = -2D_1\bar{\triangle}^2|\bar{j}|\bar{J_{ij}}, \tag{13}$$

$$\tau^u_{kk} = 2Y_1\bar{\rho}\bar{\triangle}^2|\tilde{S^u}|^2 \tag{14}$$

where $\bar{j}$ is the resolved electric current density.

The generalized Kolmogorov scaling subgrid model for MHD compressible turbulence [3] is

$$\tau^u_{ij} - \frac{1}{3}\tau^u_{kk}\delta_{ij} = -2C_2\bar{\rho}\bar{\triangle}^{4/3}\left(\tilde{S_{ij}} - \frac{1}{3}\tilde{S_{kk}}\delta_{ij}\right), \tag{15}$$

$$\tau^b_{ij} = -2D_2\bar{\triangle}^{4/3}\bar{J_{ij}}, \tag{16}$$

$$\tau^u_{kk} = 2Y_2\bar{\rho}\bar{\triangle}^{4/3}|\tilde{S^u}|. \tag{17}$$

The third model examined in this paper uses the local cross-helicity change instead of the energy dissipation functions. Therefore, the model based on cross-helicity [6] is defined as:

$$\tau^u_{ij} - \frac{1}{3}\tau^u_{kk}\delta_{ij} = -2C_3\bar{\rho}\bar{\triangle}^2|\tilde{f}|\left(\tilde{S_{ij}} - \frac{1}{3}\tilde{S_{kk}}\delta_{ij}\right), \tag{18}$$

$$\tau^b_{ij} = -2D_3\bar{\triangle}^2 sgn(\bar{j}\ \tilde{\omega})|\bar{j}\ \tilde{\omega}|^{1/2}\bar{J_{ij}}, \tag{19}$$

$$\tau^u_{kk} = 2Y_3\bar{\rho}\bar{\triangle}^2|\tilde{f}||\tilde{S^u}|. \tag{20}$$

Here, $\bar{S^b_{ij}} = \left(\partial\bar{B}_i/\partial x_j + \partial\bar{B}_j/\partial x_i\right)/2$, $\tilde{S_{ij}} = \left(\partial\tilde{u}_i/\partial x_j + \partial\tilde{u}_j/\partial x_i\right)/2$, $\tilde{f} = |\tilde{S_{ij}}\ \bar{S^b_{ij}}|^{1/2}$, $\tilde{\omega} = \nabla\times\tilde{u}$ is the vorticity and function $sgn(\cdot)$ determines the sign of the argument.

The scale-similarity model can be calculated in a LES by means of the filtered variables in contrast to other models. The scale-similarity model for MHD compressible case [6] is written in the following manner:

$$\tau^u_{ij} = \bar{\rho}\left(\widetilde{\tilde{u}_i\tilde{u}_j} - \tilde{u}_i\tilde{u}_j\right) - \frac{1}{M_a^2}\left(\overline{\bar{B}_i\bar{B}_j} - \bar{\bar{B}}_i\bar{\bar{B}}_j\right) \tag{21}$$

$$\tau^b_{ij} = \left(\overline{\tilde{u}_i\bar{B}_j} - \tilde{\tilde{u}}_i\bar{\bar{B}}_j\right) - \left(\overline{\bar{B}_i\tilde{u}_j} - \bar{\bar{B}}_i\tilde{\tilde{u}}_j\right). \tag{22}$$

The mixed model for MHD compressible turbulence is a combination of two models: the scale similarity and the Smagorinsky models for MHD case [6]:

$$\tau^u_{ij} - \frac{1}{3}\tau^u_{kk}\delta_{ij} = -2C_5\bar{\rho}\bar{\triangle}^2|\tilde{S^u}|\left(\tilde{S_{ij}} - \frac{\delta_{ij}}{3}\tilde{S_{kk}}\right) + \bar{\rho}\left(\widetilde{\tilde{u}_i\tilde{u}_j} - \tilde{\tilde{u}}_i\tilde{\tilde{u}}_j\right) - \frac{1}{M_a^2}\left(\overline{\bar{B}_i\bar{B}_j} - \bar{\bar{B}}_i\bar{\bar{B}}_j\right) \tag{23}$$

$$\tau^b_{ij} = -2D_5\bar{\triangle}^2|\bar{j}|\bar{J_{ij}} + \left(\overline{\tilde{u}_i\bar{B}_j} - \tilde{\tilde{u}}_i\bar{\bar{B}}_j\right) - \left(\overline{\bar{B}_i\tilde{u}_j} - \bar{\bar{B}}_i\tilde{\tilde{u}}_j\right) \tag{24}$$

$$\tau^u_{kk} = 2Y_5\bar{\rho}\bar{\triangle}^2|\tilde{S^u}|^2. \tag{25}$$

The parameters C_k, Y_k, and D_k ($k = 1, 2, 3$ or 5) are model constants, their values being self-consistently computed during run time with the help of the dynamic procedure that has been described in detail in the literature [10,15] and has been applied for MHD flows [3,16].

3 Aspects of numerics

The numerical method and finite-difference scheme used for computations are described in this section.

In present work, numerical code of the fourth order of accuracy for MHD equations written in the conservative form is used. The skew-symmetric form is applied for the nonlinear terms, because the skew-symmetric form of the equation is a form obtained by averaging divergence form and convective form of the nonlinear term. In spite of analytical equivalence of all the three of these forms, their numerical computations give different results. To reduce error of discretization when finite difference scheme is used and to improve computational accuracy the skew-symmetric discretization is applied for nonlinear terms [18].

For numerical solution of system of MHD equations, in this work we use the numerical code based on non-spectral finite-difference schemes. To separate the turbulent flow into large and small eddy components, Gaussian filter of the fourth order of accuracy is applied. Sagaut and Grohens [19] investigated the optimal discrete forms of Gaussian filter and top-hat filter for central finite-difference scheme of various order of accuracy in detail. One-dimensional filter is written in the following way (for x-direction):

$$\bar{\zeta}_i = \frac{\epsilon^4 - 4\epsilon^2}{1152}(\zeta_{i-2} + \zeta_{i+2}) + \frac{16\epsilon^2 - \epsilon^4}{288}(\zeta_{i-1} + \zeta_{i+1}) + \frac{\epsilon^4 - 20\epsilon^2 + 192}{192}\zeta_i, \tag{26}$$

where ζ_i is the flow parameter at point i and parameter ϵ represents the ratio of the mesh size to the cut-off lengthscale of the filter [19].

Since the compressible turbulence considered in this work is three-dimensional, three dimensional filter must be used. Sagaut and Grohens [19] showed that multidimensional filter constructed by sequential product of one-dimensional ones gives more accurate results in comparison with linear combination of one-dimensional filters. Therefore, in this work the sequential product of filters is employed for three-dimensional filtering:

$$\xi^n = \prod_{i=1}^{n} \xi^i, \tag{27}$$

where ξ^i is the one-dimensional filter in direction i and n is the space dimension.

The results obtained by LES are compared with DNS computations and performance of LES is examined by difference between LES- and filtered DNS-results. The initial conditions for LES are obtained by filtering the initial conditions of DNS. The initial velocities and magnetic fields are chosen to resemble a MHD mixing layer by adapting the hydrodynamic case. The initial condition is generated by the hyperbolic tangent profiles, and the uniform noise is used to perturb the initial mean flow (multiplied by $\sim\exp(-x_i/4)$, since the exponential term guarantees that disturbances decay in the free stream). The shear for velocity and magnetic field in the initial conditions is given z-coordinate depending. The initial conditions are held non-zero skewness of the velocity and the magnetic field. The Courant–Friedrichs–Levy stability condition (CFL-condition) is imposed on the time step. The uniform mesh with 64^3 grid cells is used for LES and 256^3 for DNS. Test computations and comparison of the results obtained by using different types of closures are carried out for various similarity parameters. For time integration the third order low-storage Runge–Kutta method is used. Periodic boundary conditions for all the three dimensions are applied, the simulation domain is a cube with dimensions of $2\pi \times 2\pi \times 2\pi$.

The model constants in SGS closures are determined by means of the dynamic procedure and test filter with filter width twice as large as initial one is used.

4 Numerical results and discussions

In this section, results of compressible MHD modeling obtained by LES approach with the use of various SGS parameterizations are represented. On the basis of comparison of LES results with results of numerical experiments performed by DNS the analysis of temporal dynamics of the skewness and the flatness is made.

Direct numerical simulation calculations are performed on the sufficient grid refinement so that accuracy of the obtained results has reflected real dynamics of three-dimensional compressible MHD turbulence and has allowed to compare to LES calculations. In the series numerical experiments given in this work the following basic parameters describing charged flow fluid are varied: magnetic Reynolds number Re_m, hydrodynamic

Reynolds number Re, Mach number M_s, and Taylor Reynolds number Re_λ. The quantity Re_λ is defined through the Taylor length microscale λ:

$$\lambda^2 = 15\mu U^2/\rho\varepsilon \tag{28}$$

$$Re_\lambda = U\lambda\rho/\mu \tag{29}$$

where U is the root-mean-square value of the velocity, ε is the rate of energy dissipation.

Initial parameters for all numerical computations performed in this work for studying of compressible MHD turbulence are the followings: $M_a = 0.6$ is the magnetic Mach number, $\gamma = 5/3$ is the polytropic index, $U = 0.608$ is the rms value of the velocity, $\beta = 0.246$ is the rms value of the magnetic field. Other parameters vary and numerical cases of modeling of compressible MHD turbulence considered in this paper have the following ranges of change of similarity numbers: sonic Mach number varies over the range $M_s \in [0.2; 1]$, hydrodynamics Reynolds number has the boundaries $Re \in [100; 4050]$ (respectively for Taylor Reynolds number $Re_\lambda \in [25; 165]$), and magnetic Reynolds number is confined within the range $Re_m \in [2; 20]$. Initial data for all numerical calculations performed in the present work are represented in Table 1 for sake of clarity.

Large eddy simulation method is carried out for five SGS models formulated previously. For the sake of convenience following notations are introduced. The notation M0 corresponds to the case when tensors τ_{ij}^u and τ_{ij}^b are simply omitted, which means that LES, in fact, is DNS on the coarse LES-grid starting from filtered initial conditions. The case M0 (solid line) is included here for a more detailed analysis and understanding of an influence SGS parameterizations on the modeling of MHD fluid flow for comparison DNS results with LES results made by various SGS closures (M1–M5). The notation M1 denotes the Smagorinsky model for MHD turbulence (dashed line), M2 is the Kolmogorov model for MHD case (dotted line), M3 is the model based on cross-helicity (black point line), M4 is the scale-similarity model for MHD flow (marker+), and M5 represents the mixed model for MHD case (dashed-dot line). The DNS results are represented by the diamond line. For clarity the notations of DNS and LES results used in the present paper are listed in Table 2.

In Figs. 1 and 2 numerical results of time evolution of the skewness and the flatness for the case #1, when $Re = 100$, $Re_\lambda = 25$, $Re_m = 10.0$, $M_s = 0.6$ are presented and time dynamics of the skewness and the flatness for the case #2 ($Re = 4050$, $Re_\lambda = 165$, $Re_m = 10.0$, $M_s = 0.6$) are shown in Figs. 3 and 4. Note that the change of Reynolds number virtually do not have an effect on the skewness of the velocity and magnetic field components. This conclusion agrees with that drawn in results of article of Sreenivasan and Antonia [21] where they have compiled many experimental velocity structure function measurements and have shown that the skewness appears constant in a wide range of hydrodynamic Reynolds numbers. It is shown in work [6] that changing of Reynolds number Re_λ produces qualitatively similar results, as the initial conditions of

Table 1 Initial parameters for study of compressible MHD turbulence

Case	λ	Re	Re_m	Re_λ	M_s	M_a	κ	μ	γ	U	β
#1	0.843	100	10.0	25	0.6	0.6	0.108	0.020	5/3	0.608	0.246
#2	0.843	4050	10.0	165	0.6	0.6	0.024	0.001	5/3	0.608	0.246
#3	0.843	390	10.0	50	0.2	0.6	0.077	0.010	5/3	0.608	0.246
#4	0.843	390	10.0	50	1	0.6	0.077	0.010	5/3	0.608	0.246
#5	0.843	390	2.00	50	0.6	0.6	0.077	0.010	5/3	0.608	0.246
#6	0.843	390	20.0	50	0.6	0.6	0.077	0.010	5/3	0.608	0.246

λ Taylor microscale, Re_λ Taylor Reynolds number, Re hydrodynamic Reynolds number, Re_m magnetic Reynolds number, M_s Mach number, M_a magnetic Mach number, κ Kolmogorov scale, μ coefficient of molecular viscosity, γ polytropic index, U rms value of the velocity, β rms value of the magnetic field

Table 2 Notation for DNS and LES results using various subgrid-scale models

Notation	Results	Curve
	DNS	Diamond
M0	No model	Solid
M1	Smagorinsky model	Dashed
M2	Kolmogorov model	Dotted
M3	Cross-helicity model	Black point
M4	Scale-similarity model	Marker+
M5	Mixed model	Dashed-dot

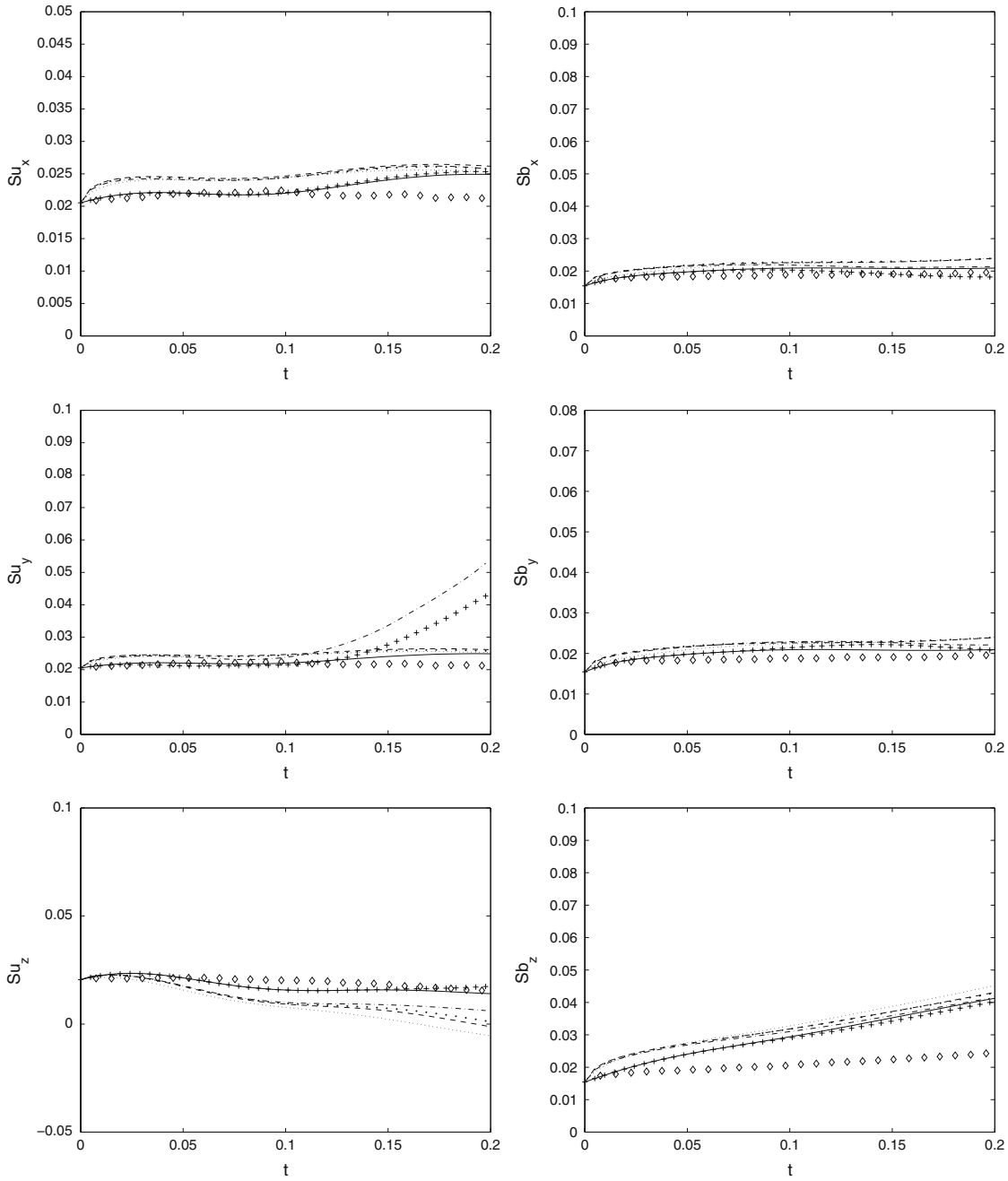

Fig. 1 Time dynamics of skewness of the velocity and the magnetic field components for the case #1 when $Re = 100$, $Re_\lambda = 25$, $Re_m = 10.0$, $M_s = 0.6$. See Table 2 for notations

velocity and magnetic fields are the same. Therefore Taylor Reynolds number does not have a significant impact on the choice of subgrid parametrization in our computations. The SGS closures: M1, M2, M3, M5 models show adequate results and good approximations to DNS. It is apparent from Fig. 1 that for the skewness y-component of the velocity, the SGS models M4 and M5 (M4 enters as one of term in the model M5) show inadequate results and have maximum deviation from "exact" DNS-results. Perhaps, it is related to the fact that the definition of M4 model implies that the SGS model only takes into account the contribution of the filtered variables to the turbulent SGS stresses. The largest divergence from DNS results is demonstrated by the model M2 for the skewness z-component of the velocity. It is probably connected with formulation of M2 model because it is supposed that the filter is in the inertial range and the energy dissipation rate is spatially

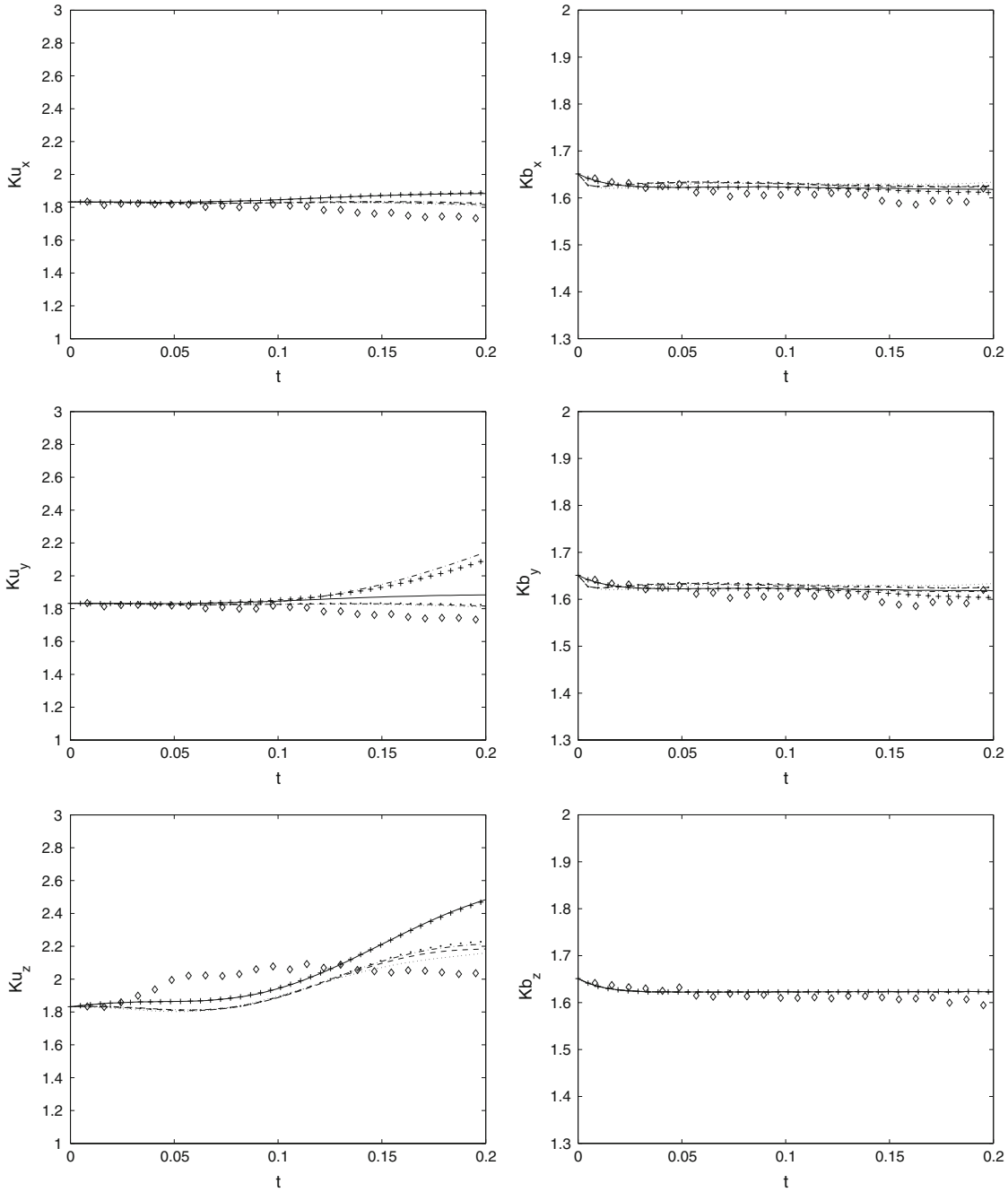

Fig. 2 Time dynamics of flatness of the velocity and the magnetic field components for the case #1 when $Re = 100$, $Re_\lambda = 25$, $Re_m = 10.0$, $M_s = 0.6$. See Table 2 for notations

constant in that range. For the skewness z-component of the velocity and for the skewness components of the magnetic field, an essential difference in numerical results of various subgrid closures is not present under various Reynolds numbers and the best results provide models M0 and M4. The flatness factor of the velocity increases gradually with Reynolds number because a fluid flow becomes more and more turbulent with increase in hydrodynamic Reynolds number. It is observed that SGS closures M4 and M5 display incorrect results for the flatness of y-component of the velocity as well as for the skewness, while the models M1–M3 improve calculation accuracy. The SGS parametrization M0 and M4 shows upper deviation for the flatness x- and z-components of the velocity. For the flatness of components of the magnetic field, dependence on a

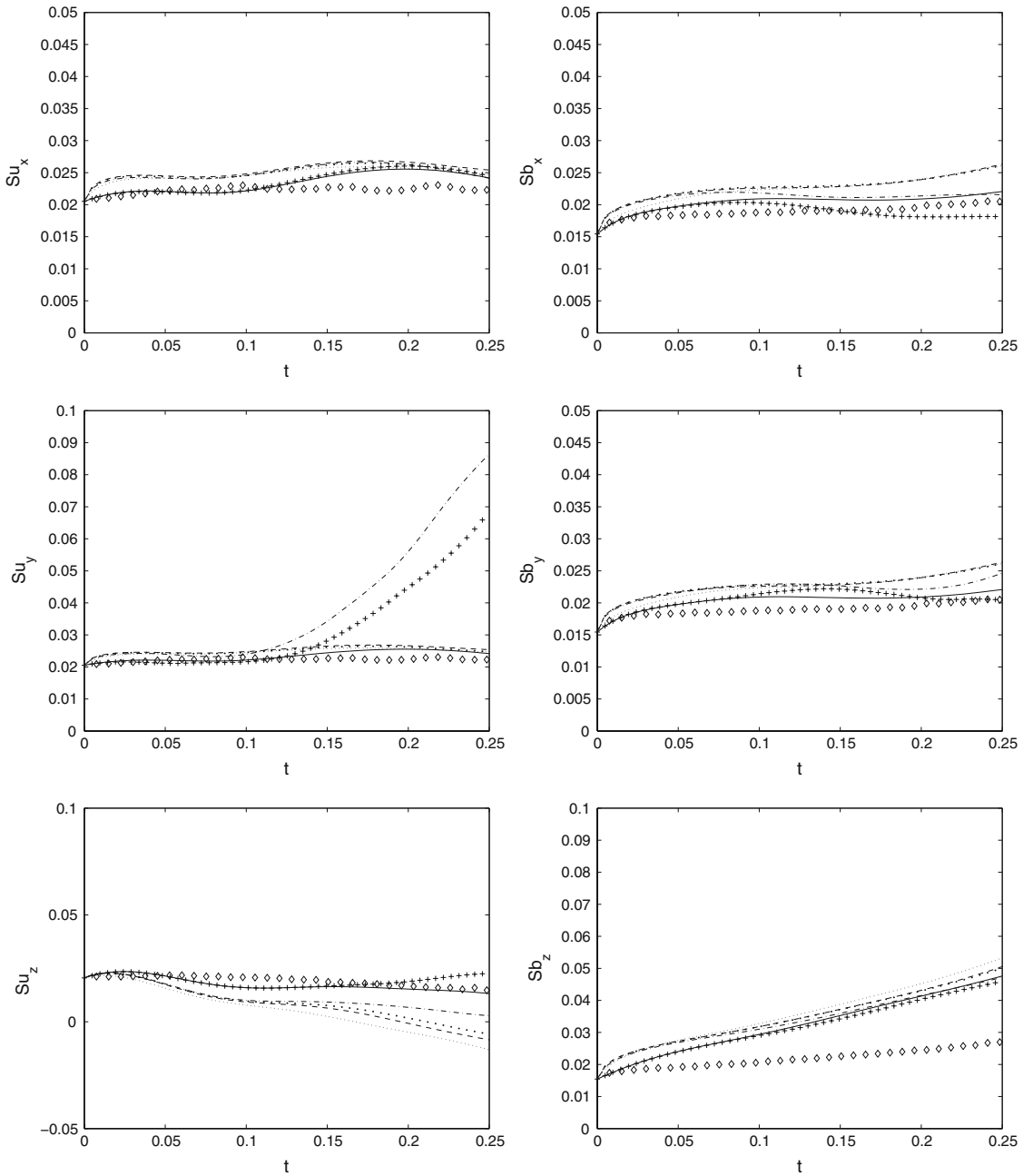

Fig. 3 Time dynamics of skewness of the velocity and the magnetic field components for the case #2 when $Re = 4050$, $Re_\lambda = 165$, $Re_m = 10.0$, $M_s = 0.6$. See Table 2 for notations

choice SGS models is actually lacking and the numerical results of the case #1 and the case #2 for the flatness of the magnetic field are almost identical. In other words, the lack of energy dissipation for the magnetic energy in M0 and the energy pile-up at the smallest resolved scales do not practically have an effect on determination of statistical characteristics, namely, the flatness and the skewness. For two-point PDF in the Elsässer variables, the results indicate as well that M0 case without any subgrid modeling describes PDF well enough [16].

The next series of the numerical experiments are performed under various sonic Mach numbers, namely, for the case #3 ($Re = 390$, $Re_\lambda = 50$, $Re_m = 10.0$, $M_s = 0.2$) and for the case #4 ($Re = 390$, $Re_\lambda = 50$, $Re_m = 10.0$, $M_s = 1.0$). Mach number M_s exerts essential influence on results of modeling as shown in the work [6]. The divergence between DNS and LES results for kinetic energy increases with M_s. The models M2 and M3 yield the best accordance with DNS under various Mach numbers. The deviations in results for the

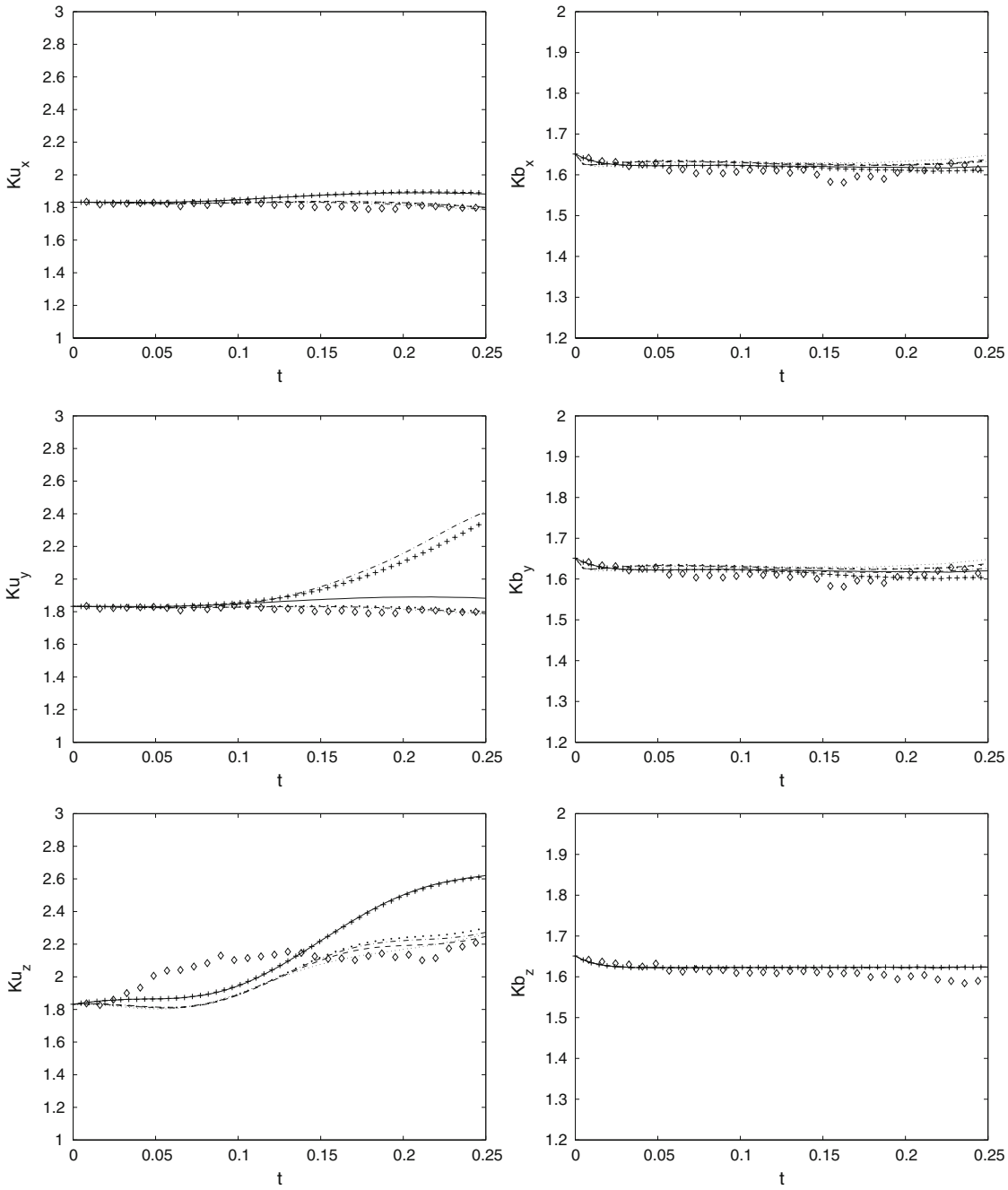

Fig. 4 Time dynamics of flatness of the velocity and the magnetic field components for the case #2 when $Re = 4050$, $Re_\lambda = 165$, $Re_m = 10.0$, $M_s = 0.6$. See Table 2 for notations

magnetic energy, on the contrary, decrease with increasing M_s. It is necessary to notice that magnetic energy reaches a stationary level more rapidly with reducing Mach number. The model M2 shows the best results both for high and for low Mach numbers for cross-helicity [6]. Time dynamics of the skewness and the flatness for the case #3 is shown in Figs. 5 and 6. In Figs. 7 and 8, time evolution of the skewness and the flatness, respectively, are demonstrated for the case #4. We observe a strong dependence of the skewness and the flatness on M_s. In these figures one can see that the skewness of the velocity when the Mach number $M_s = 1.0$ grows much more slowly than at $M_s = 0.2$. However, the agreement between DNS and LES results increases with Mach number and LES results are more exact at high Mach numbers. Perhaps, it is related to the fact that there

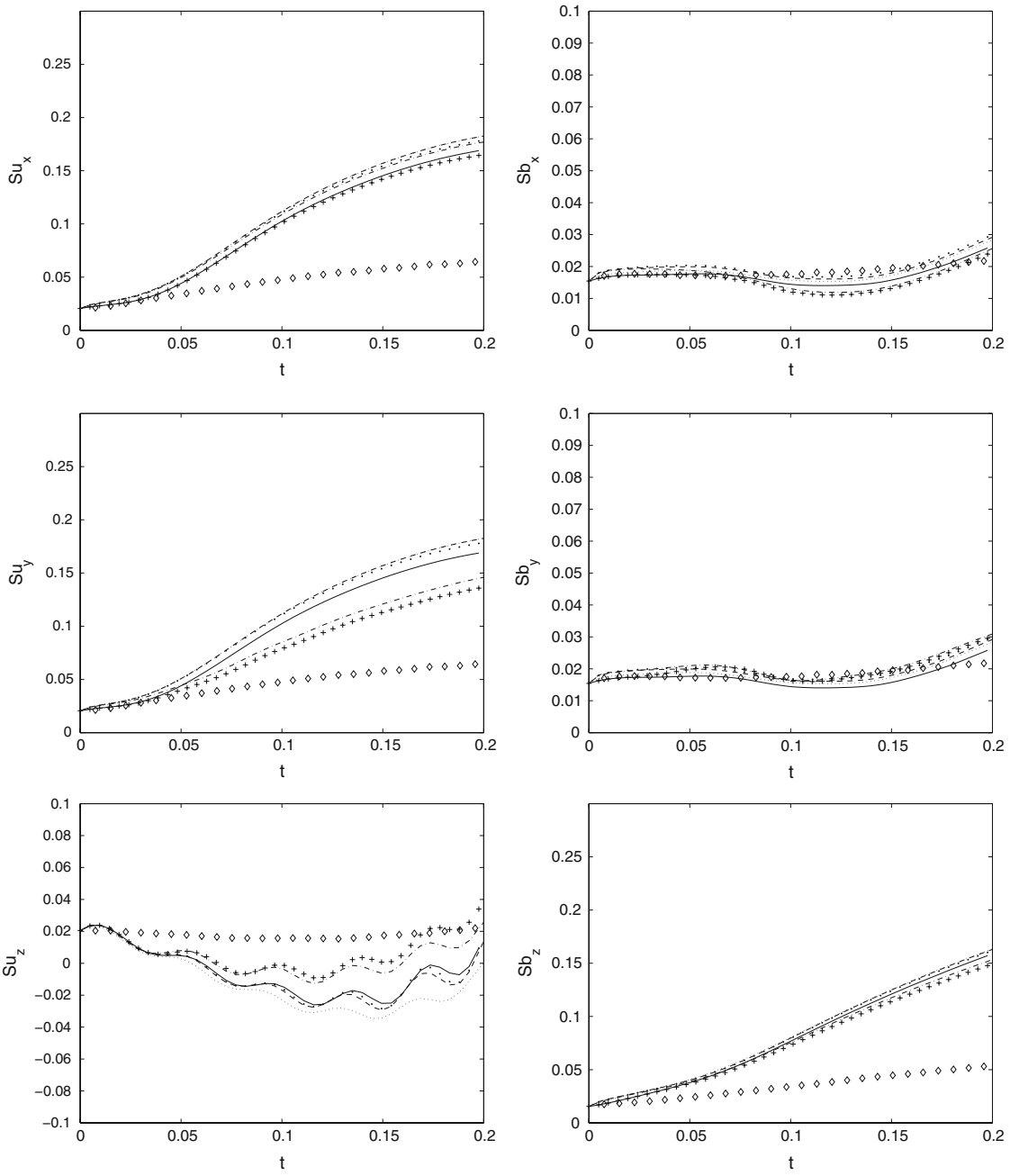

Fig. 5 Time dynamics of skewness of the velocity and the magnetic field components for the case #3 when $Re = 390$, $Re_\lambda = 50$, $Re_m = 10.0$, $M_s = 0.2$. See Table 2 for notations

can be discontinuities at $M_s = 1.0$ and a role of small-scale turbulence decreases. It is necessary to notice, that if the SGS models M0, M4, and M5 for the case #3 are the closest to DNS results, then for the case #4 these SGS models are the least exact. For the skewness of the magnetic field, as well as for velocity, the reduction of the skewness values for $M_s = 1.0$ is observed in comparison with the weakly compressible case $M_s = 0.2$ and the discrepancy between DNS and LES results decreases. The flatness of the velocity grows more strongly with increasing Mach number. If the flatness of x- and y-components remains approximately at a constant level with time at $M_s = 0.2$, then the flatness for all three components of the velocity increases with time for the case $M_s = 1.0$. The divergence between numerical results of the SGS parameterizations increases with the Mach number for the flatness. The closures M4 and M5 demonstrate incorrect results for the flatness of

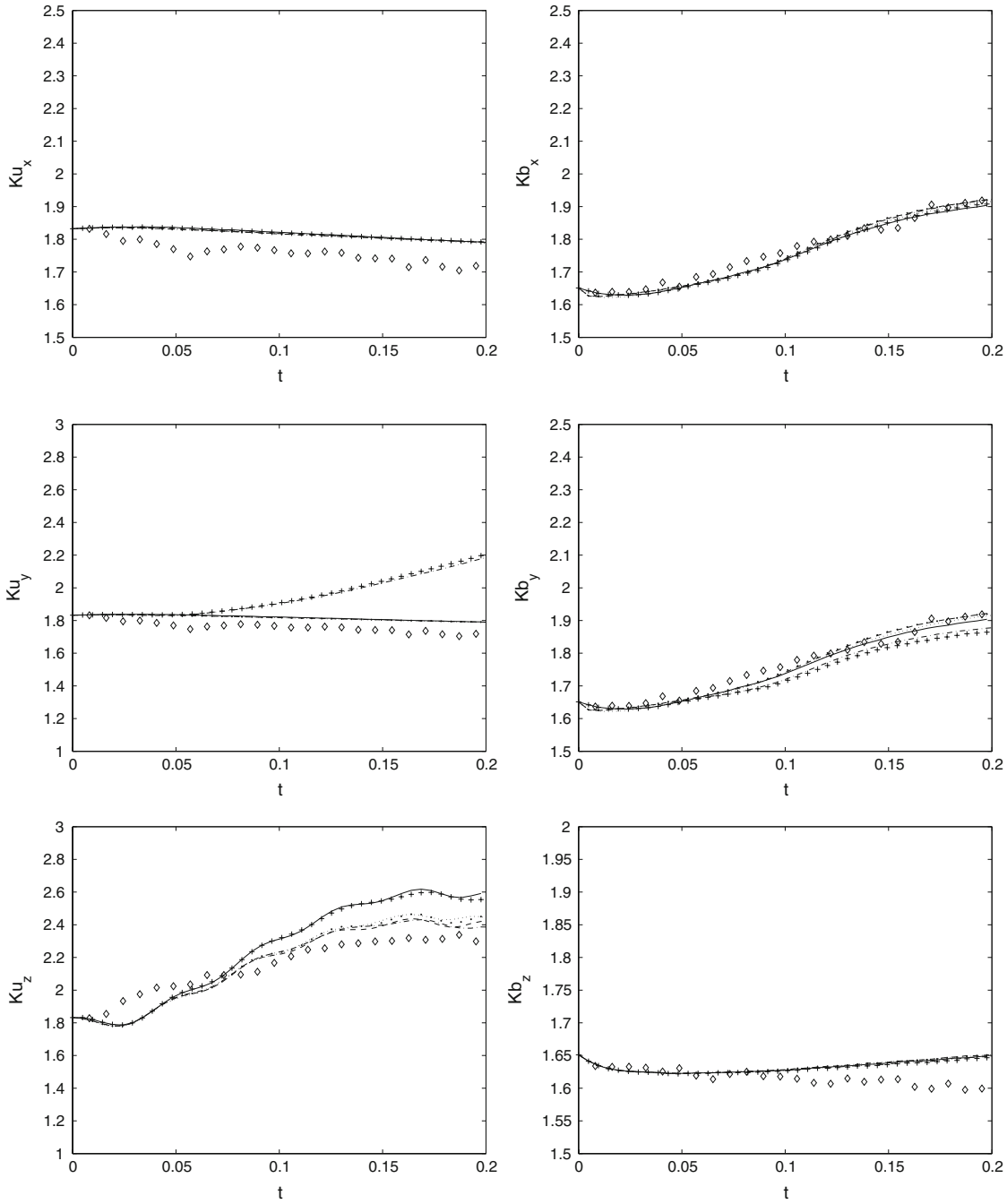

Fig. 6 Time dynamics of flatness of the velocity and the magnetic field components for the case #3 when $Re = 390$, $Re_\lambda = 50$, $Re_m = 10.0$, $M_s = 0.2$. See Table 2 for notations

y-component of the velocity owing to strong growth after $t = 0.15$. The flatness of the magnetic field behaves completely different at low and high Mach numbers. As indicated in Fig. 6, the flatness of the magnetic field grows for weakly compressible MHD flow, though decreases with time at $M_s = 1.0$ (Fig. 8). It is possible to note that the presence of SGS models does not exert influence appreciably on accuracy of the numerical results of the flatness of the magnetic field. In this case the model M0 also describes well enough time dynamics of the flatness. The different behavior of the flatness and the skewness depending on a component of the velocity and the magnetic field is connected with initial conditions because the shear is carried out on z-coordinate.

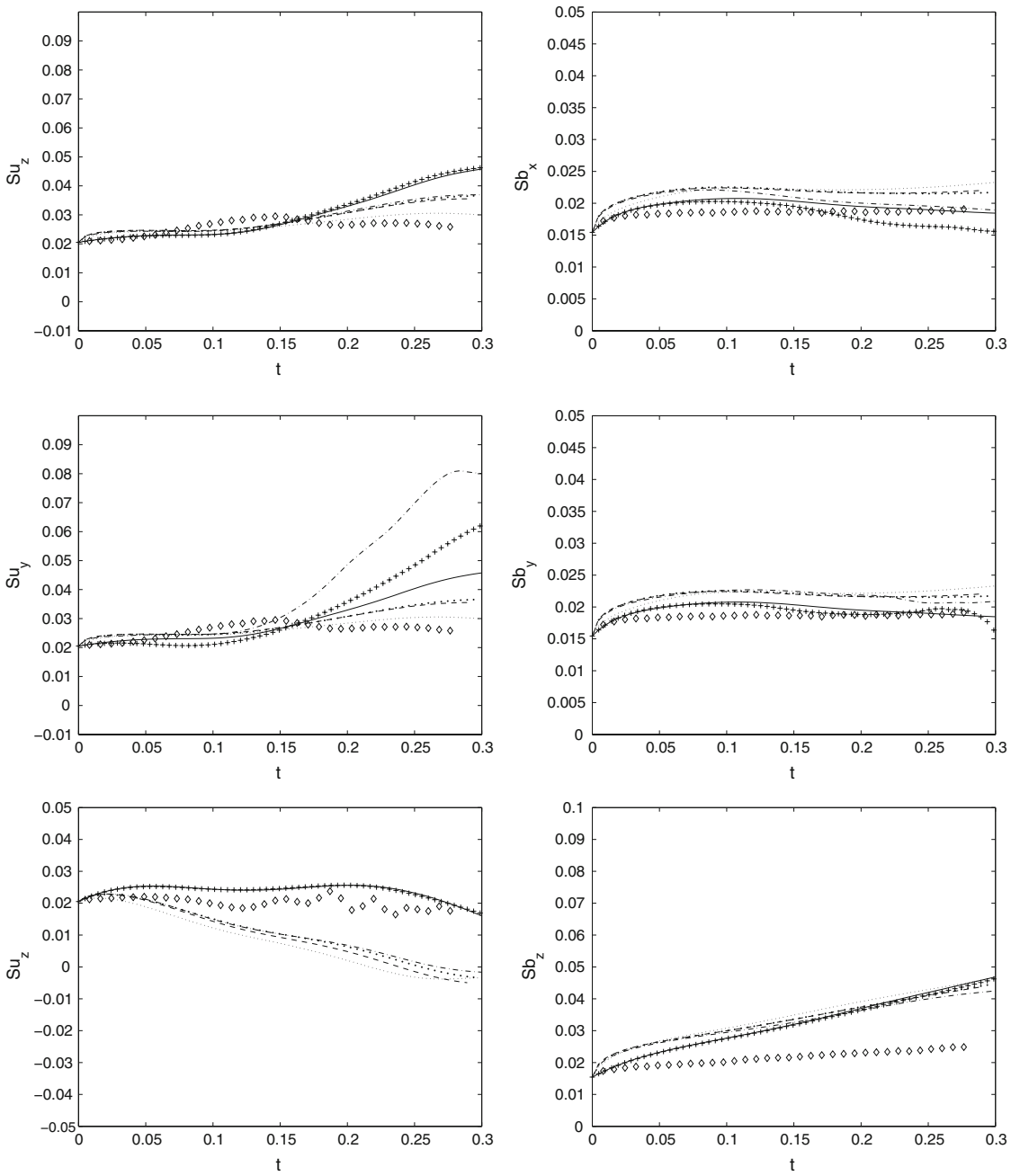

Fig. 7 Time dynamics of skewness of the velocity and the magnetic field components for the case #4 when $Re = 390$, $Re_\lambda = 50$, $Re_m = 10.0$, $M_s = 1.0$. See Table 2 for notations

In the present paper, behavior of the skewness and the flatness of the velocity and the magnetic field components and influence of subgrid parameterizations on their values are also considered under various magnetic Reynolds numbers. Following cases are discussed: the case #5 when $Re = 390$, $Re_\lambda = 50$, $Re_m = 2.0$, $M_s = 0.6$ (numerical results obtained by DNS and LES are displayed in Figs. 9 and 10), and the case #6 when $Re = 390$, $Re_\lambda = 50$, $Re_m = 20.0$, $M_s = 0.6$ (the results of temporal evolution of the skewness and the flatness are shown in Figs. 11 and 12). According to the work [6], the differences between SGS models for magnetic energy were shown to decrease with reducing magnetic Reynolds number and all models discussed above demonstrate good agreement with DNS results at small value of number Re_m. The effect of SGS closures increases with magnetic Reynolds number for modeling of compressible MHD turbulence, but rate

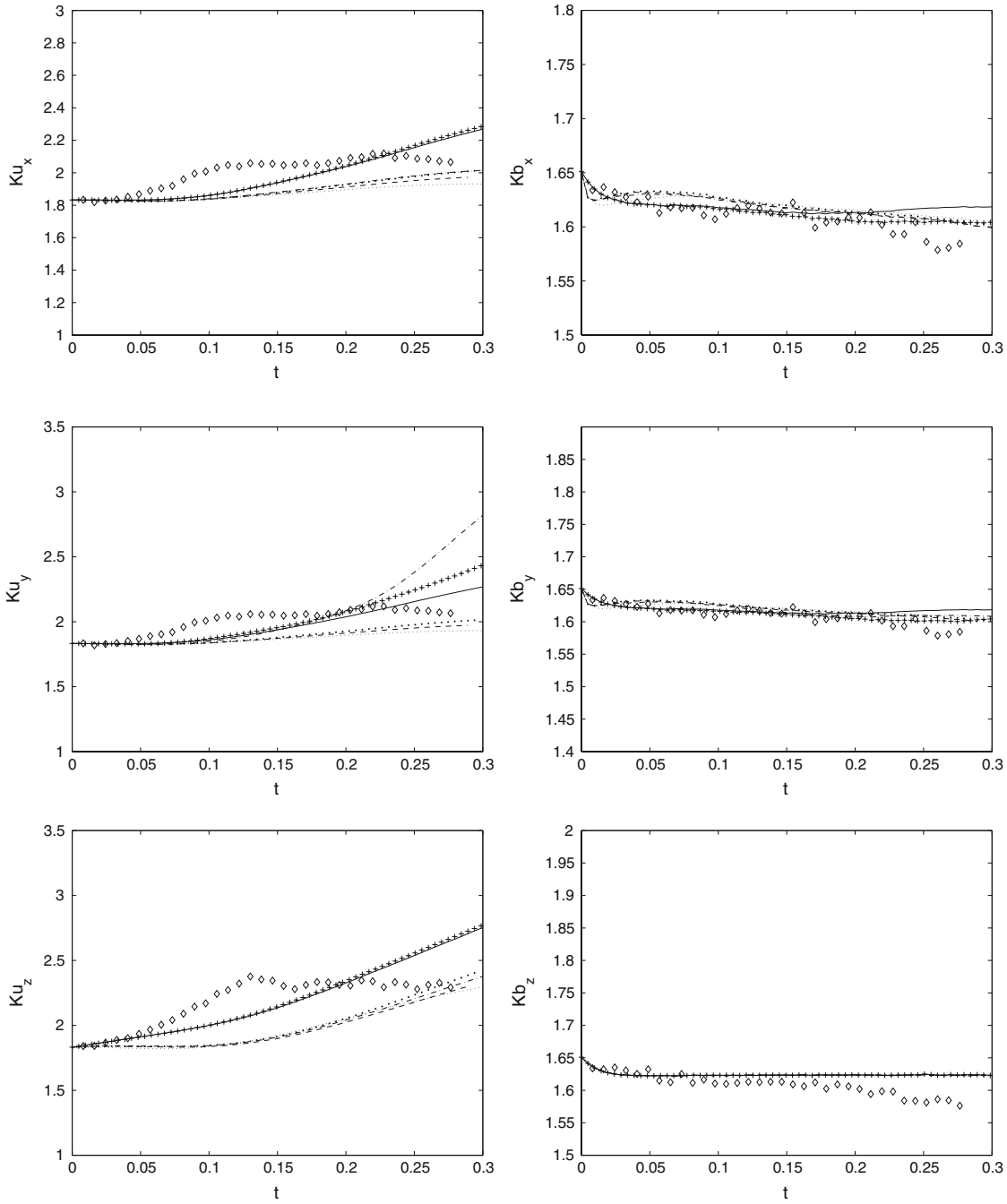

Fig. 8 Time dynamics of flatness of the velocity and the magnetic field components for the case #4 when $Re = 390$, $Re_\lambda = 50$, $Re_m = 10.0$, $M_s = 1.0$. See Table 2 for notations

of dissipation of the magnetic energy decreases with increasing Re_m. The best results for time evolution of the magnetic energy are shown by M1, M2, and M3 models. The same behavior of graphs was observed for the cross-helicity: the influence of SGS parameterizations increases with Re_m. For the kinetic energy, larger divergence of LES results was observed with decrease in magnetic Reynolds number using various SGS closures. The model M4 shows the worst results, however, the other SGS closures increase calculation accuracy [6]. There is strong dependence of the skewness and the flatness on Re_m. As illustrated in Figs. 9 and 11 for the skewness, the skewness of the velocity components decreases with increasing magnetic Reynolds number while the agreement between DNS and LES results enhances. Similar conclusions can be made for the skewness

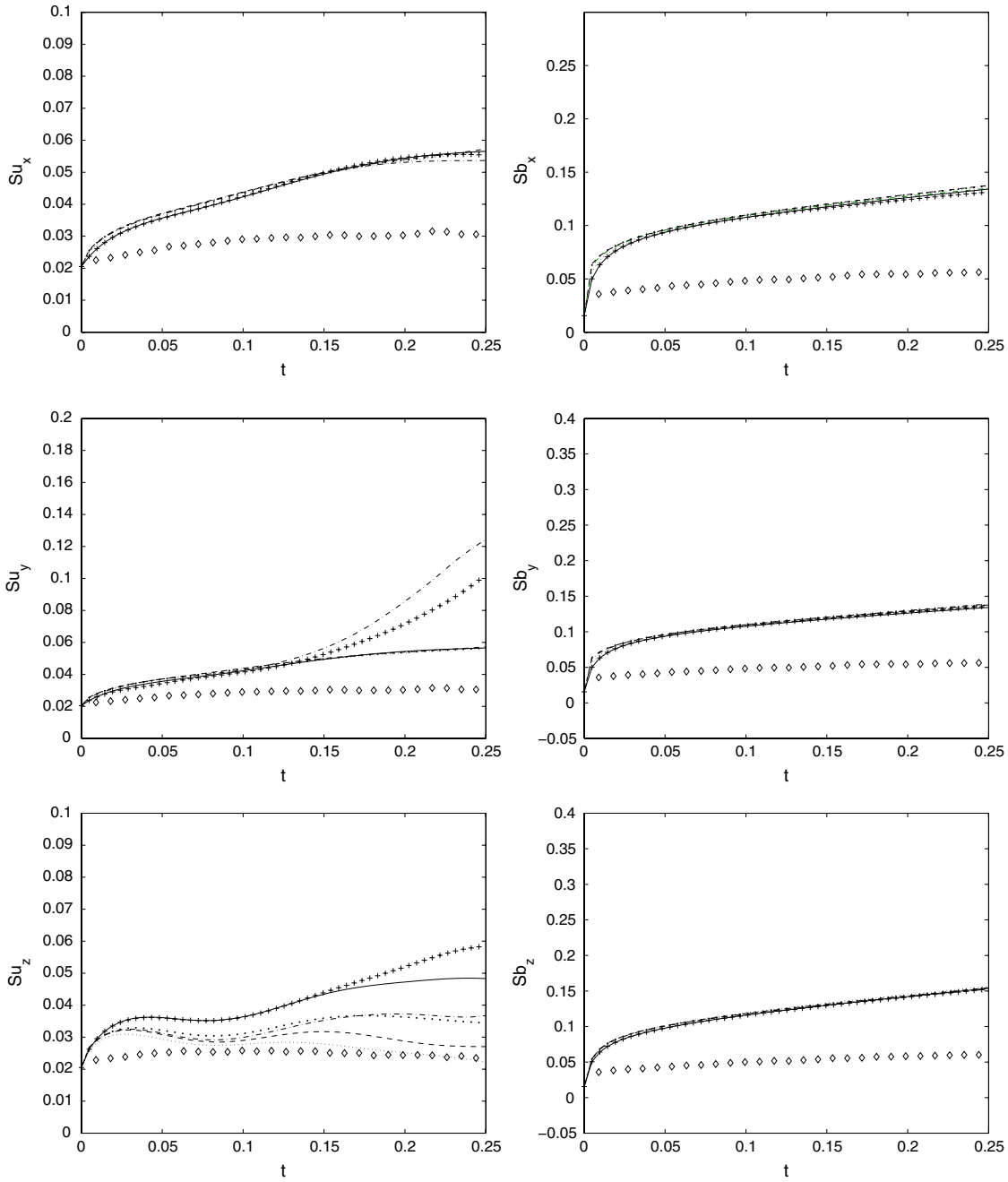

Fig. 9 Time dynamics of skewness of the velocity and the magnetic field components for the case #5 when $Re = 390$, $Re_\lambda = 50$, $Re_m = 2.0$, $M_s = 0.6$. See Table 2 for notations

of the magnetic field because calculation accuracy of LES results in comparison with DNS ones increases with magnetic Reynolds number and rise of the skewness of the magnetic field components decreases. The least exact results for the skewness of the velocity and the magnetic field are demonstrated by SGS models M0, M4, and M5 since M0 and M4 have excessively strong deviations from DNS results for z-component of the velocity for the case #5 and closures M4 and M5 for y-component of the velocity for the case #5 and #6. It is clear from Figs. 10 and 12, that in our computations the flatness of the velocity and the magnetic field are weakly affected by magnetic Reynolds number and time dynamics does not change strongly. However, the agreement between DNS and LES results increases with Re_m. From all SGS parameterizations for compressible MHD turbulence considered in this paper, in general, the most exact numerical results are shown by the SGS models

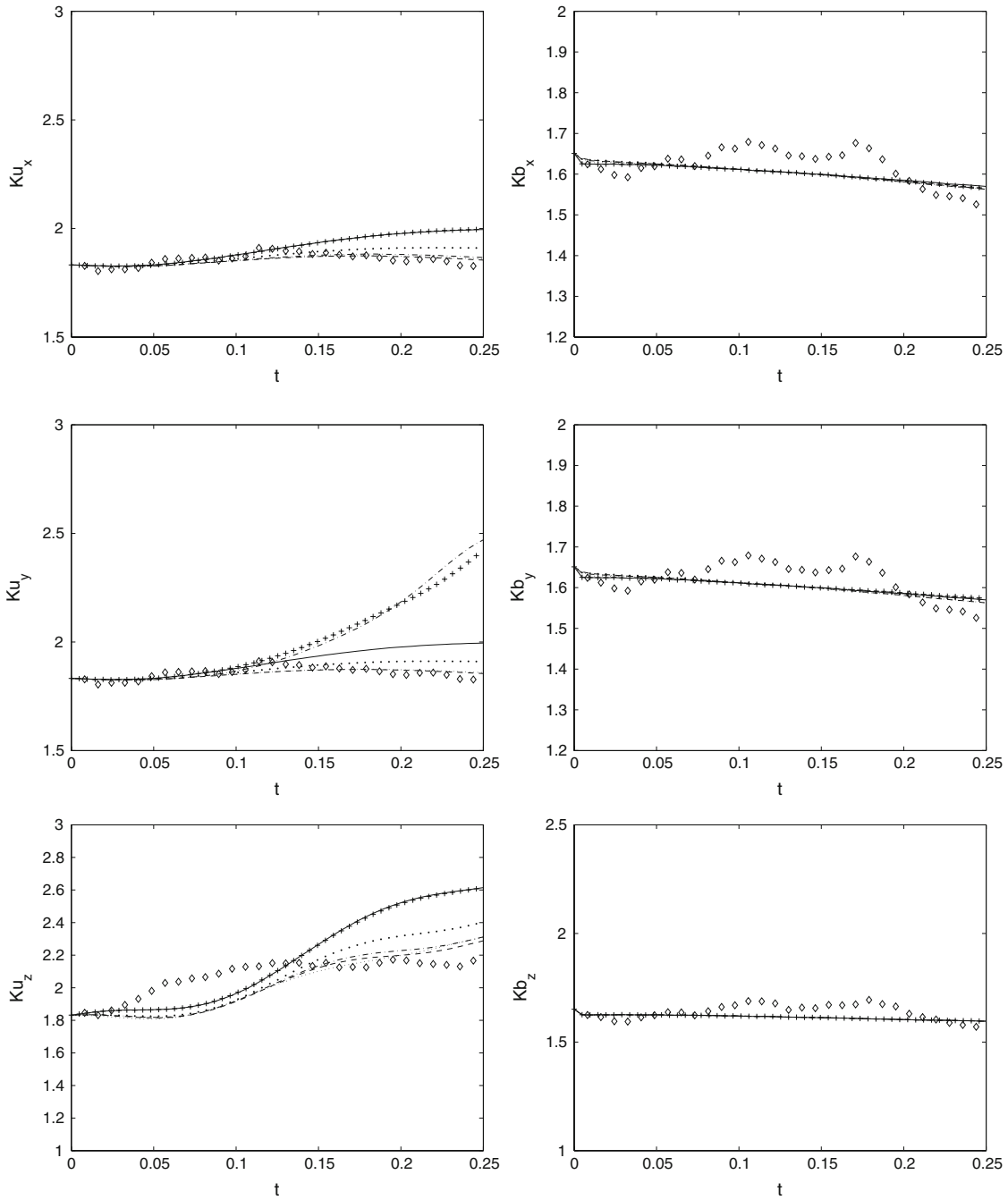

Fig. 10 Time dynamics of flatness of the velocity and the magnetic field components for the case #5 when $Re = 390$, $Re_\lambda = 50$, $Re_m = 2.0$, $M_s = 0.6$. See Table2 for notations

M1 and M3. The best results are demonstrated by M1 and M2 models, this can be associated with the fact that parametrization M3 is purely MHD model and this subgrid closure M3 is physically linked to the local energy variations caused by the relative field topology scrambling of velocity and magnetic field (turbulent motions lead to changes in the local alignment of the vectors of the velocity and the magnetic field [17]). In the SGS model M1 an analog of flow field shear is shear in the magnetic field which is the electric current and energy dissipation rate is not constant as opposed to the model M2.

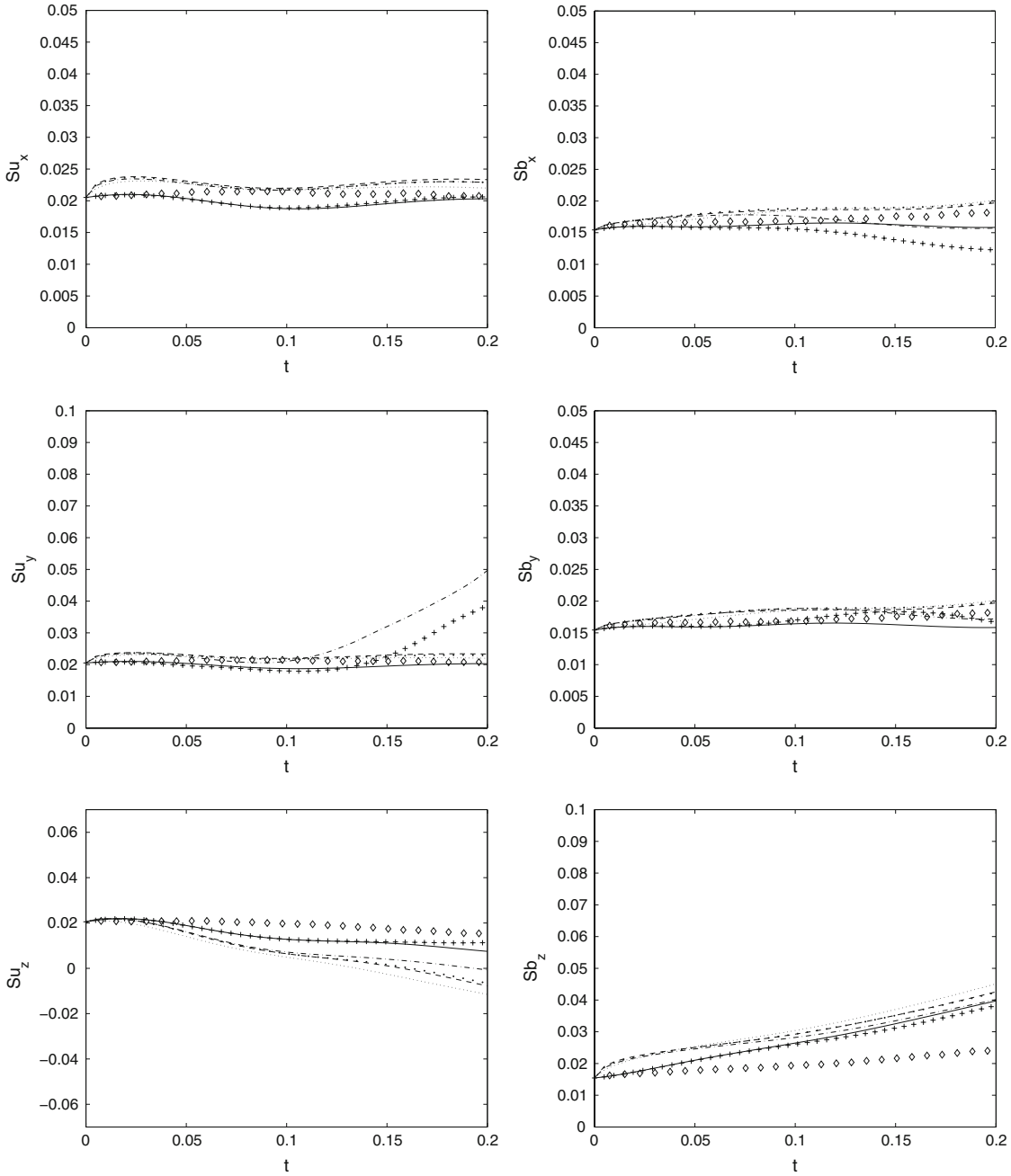

Fig. 11 Time dynamics of skewness of the velocity and the magnetic field components for the case #6 when $Re = 390$, $Re_\lambda = 50$, $Re_m = 20.0$, $M_s = 0.6$. See Table 2 for notations

5 Conclusions

In the present work, applicability of LES method for studying of non-Gaussian properties of PDF for turbulent compressible magnetic fluid flow is investigated and potential feasibilities of various SGS parameterizations by means of comparison with DNS results are explored. LES approach is effective alternative to DNS method for turbulent flow with very high Reynolds number. However, use of filtering procedure virtually excludes from calculations a small-scale part of turbulent flow on which scales most part of non-Gaussian fluctuations are displayed. For this reason potential possibilities of LES method for modeling various PDF's for turbulent flows demand additional research. The shape of the PDFs depends on the structure of the analyzed field. In LES

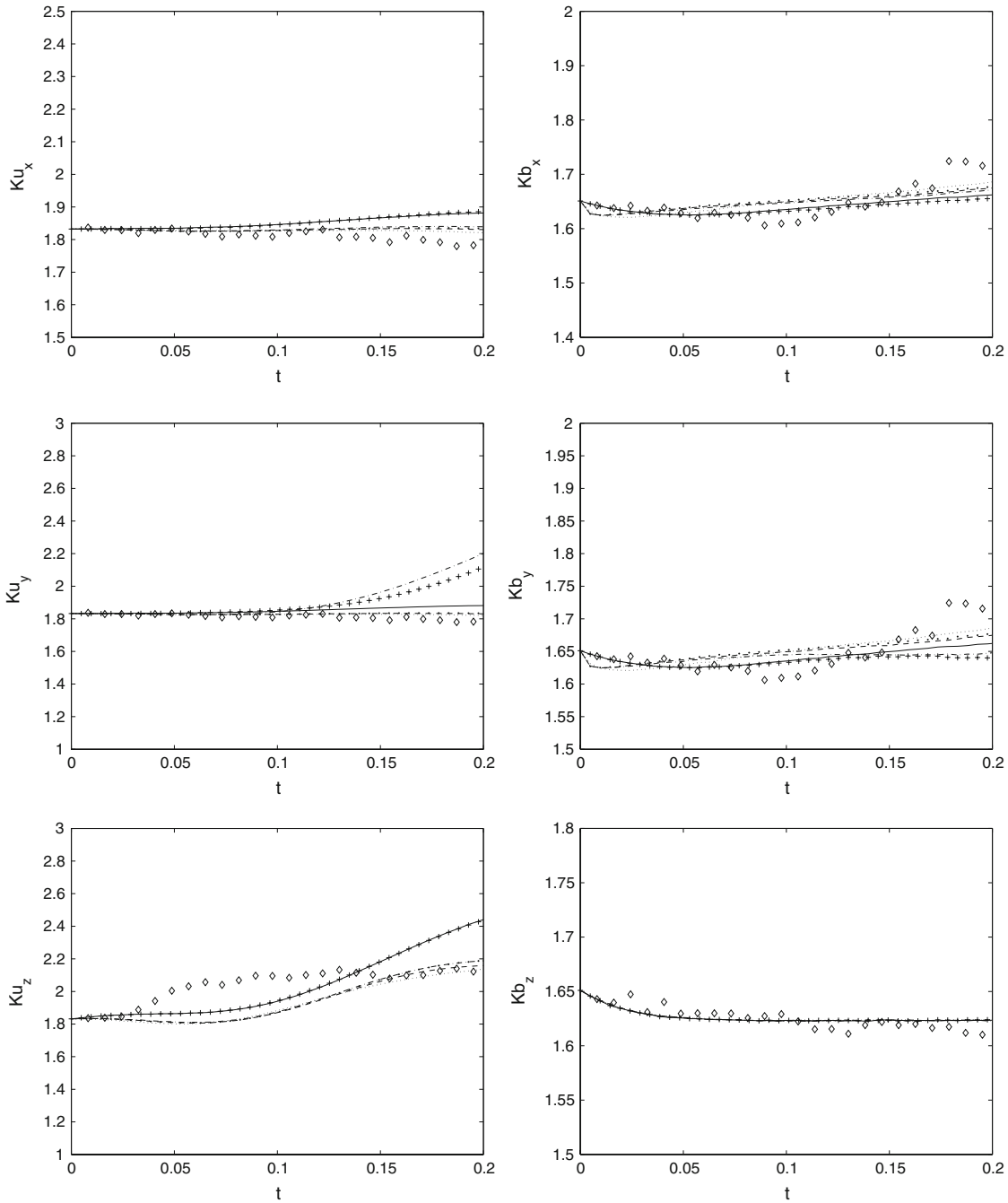

Fig. 12 Time dynamics of flatness of the velocity and the magnetic field components for the case #6 when $Re = 390$, $Re_\lambda = 50$, $Re_m = 20.0$, $M_s = 0.6$. See Table 2 for notations

method, the structure of the large eddies depends to some extent on the characteristics of the SGS parameterizations and the conclusions must always be subject to cautions. To characterize properties of PDF, the skewness and the flatness of the velocity and the magnetic field components under various hydrodynamic Reynolds numbers, sonic Mach numbers and magnetic Reynolds numbers are studied in our work. The skewness and the flatness of turbulent motion are the important parameters for understanding of structure of turbulent MHD flow, statistical properties of charged fluid under consideration. Numerical study is performed using five various SGS closures: the Smagorinsky model, the Kolmogorov model, the cross-helicity model, the scale-similarity model, and mixed model for MHD case.

Efficiency is demonstrated by various SGS models depends on similarity numbers of turbulent MHD flow. It should be noted that, in general, lack of dissipation in LES model without any SGS parametrization for kinetic and magnetic energies does not have an effect on determination of the skewness and the flatness, the case without any subgrid modeling sometimes lies even closer to the DNS results. This indicates that the energy pile-up at the small scales, that is characteristic for the case without any SGS closure, does not significantly influence determination of PDF. It is shown that, in general, among the subgrid models, the best results for studying of the flatness and the skewness of the velocity and the magnetic field components are demonstrated by the Smagorinsky model for MHD turbulence and the model based on cross-helicity for MHD case.

It is visible from the numerical results that the SGS parametrization choice for the flatness and the skewness of the velocity is more essential than for the same characteristics of the magnetic field. In consequence of the investigation carried out, it is shown that LES method provides adequate results and LES technique may be used for the study of PDF characteristics (for instance, structural functions of various moments of velocity and magnetic field) of compressible MHD fluid flow at various similarity numbers.

The flatness and the skewness define properties of probability density for the turbulent process. Therefore, the obtained results concerning applicability of various subgrid parameterizations for calculation of these characteristics can be used for reconstruction of PDF based on computations by LES method.

Acknowledgements This work has been partly supported by Russian Foundation for Basic Research project 08-08-00687-a.

References

1. Agullo, O., Müller, W.C., Knaepen, B., Carati, D.: Large eddy simulation of decaying magnetohydrodynamic turbulence with dynamic subgrid-modeling. Phys. Plasmas **8**(7), 3502–3505 (2001)
2. Biskamp, D.: Magnetohydrodynamic Turbulence. Cambridge University Press, Cambridge (2003)
3. Chernyshov, A.A., Karelsky, K.V., Petrosyan, A.S.: Large-eddy simulation of magnetohydrodynamic turbulence in compressible fluid. Phys. Plasmas **13**(3), 032304 (2006)
4. Chernyshov, A.A., Karelsky, K.V., Petrosyan, A.S.: Subgrid-scale modelling in large-eddy simulations of compressible magnetohydrodynamic turbulence. Russ. J. Numer. Anal. Math. Model. **21**(1), 1–20 (2006)
5. Chernyshov, A.A., Karelsky, K.V., Petrosyan, A.S.: Subgrid-scale modelling of compressible magnetohydrodynamic turbulence in heat-conducting plasma. Phys. Plasmas **13**(10), 104501 (2006)
6. Chernyshov, A.A., Karelsky, K.V., Petrosyan, A.S.: Development of large eddy simulation for modeling of decaying compressible MHD turbulence. Phys. Fluids **19**(5), 055106 (2007)
7. Chernyshov, A.A., Karelsky, K.V., Petrosyan, A.S.: Assessment of subgrid-scale models for decaying compressible MHD turbulence. Flow, Turbul. Combust. **80**(1), 21–35 (2008). doi:10.1007/s10494-007-9100-8
8. Chernyshov, A.A., Karelsky, K.V., Petrosyan, A.S.: Modeling of compressible magnetohydrodynamic turbulence in electrically and heat conducting fluid using large eddy simulation. Phys. Fluids **20**(8), 085106 (2008)
9. Chernyshov, A.A., Karelsky, K.V., Petrosyan, A.S.: Three-dimensional modeling of compressible magnetohydrodynamic turbulence in the local interstellar medium. Astrophys. J. **686**, 1137–1144 (2008)
10. Germano, M., Piomelli, U., Moin, P., Cabot, W.: A dynamic subgrid-scale eddy-viscosity model. Phys. Fluids A **3**(7), 1760–1765 (1991)
11. Gomez, T., Sagaut, P., Schilling, O., Zhou, Y.: Large-eddy simulation of very large kinetic and magnetic reynolds number isotropic magnetohydrodynamic turbulence using a spectral subgrid model. Phys. Fluids **19**(4), 032304 (2007)
12. Jiménez, M.A., Cuxart, J.: Study of the probability density functions from a large-eddy simulation for a stably stratified boundary layer. Boundary-Layer Meteorol. **118**, 401–420 (2006)
13. Knaepen, B., Moin, P.: Large-eddy simulation of conductive flows at low magnetic reynolds number. Phys. Fluids **16**(5), 1255–1261 (2004)
14. Lazarian, A.: Intermittency of magnetohydrodynamic turbulence: astrophysical perspective. Int. J. Mod. Phys. D **15**, 1099–1111 (2006)
15. Lilly, D.: A proposed modification of the germano subgrid scale closure method. Phys. Fluids A **4**, 633–635 (1992)
16. Müller, W.C., Carati, D.: Dynamic gradient-diffudion subgrid models for incompressible magnetohydrodynamics turbulence. Phys. Plasmas **9**(3), 824–834 (2002)
17. Müller, W.C., Carati, D.: Large-eddy simulation of magnetohydrodynamic turbulence. Comput. Phys. Commun. **147**, 344–347 (2002)
18. Park, N., Yoo, J., Choi, H.: Discretization errors in large eddy simulation: on the suitability of centered and upwind-biased compact difference schemes. J. Comput. Phys. **198**, 580–616 (2004)
19. Sagaut, P., Grohens, R.: Discrete filters for large eddy simulation. Int. J. Numer. Mech. Fluids **31**, 1195–1220 (1999)
20. Smagorinsky, J.: General circulation experiments with the primitive equations. Mon. Weather Rev. **91**, 99–164 (1963)
21. Sreenivasan, K.R., Antonia, R.A.: The phenomenology of small-scale turbulence. Annu. Rev. Fluid Mech. **29**, 435–472 (1997)
22. Theobald, M., Fox, P., Sofia, S.: A subgrid-scale resistivity for magnetohydrodynamics. Phys. Plasmas **1**(9), 3016–3032 (1994)
23. Vorobev, A., Zikanov, O.: Smagorinsky constant in les modeling of anisotropic MHD turbulence. Theor. Comput. Fluid Dyn. **22**(3–4), 317–325 (2007)